

Contents lists available at ScienceDirect

Earth and Planetary Science Letters

journal homepage: www.elsevier.com/locate/epsl

Mercury emissions and stable isotopic compositions at Vulcano Island (Italy)

T. Zambardi ^{a,*}, J.E. Sonke ^a, J.P. Toutain ^a, F. Sortino ^b, H. Shinohara ^c^a Observatoire Midi-Pyrénées - Laboratoire des Mécanismes et Transferts en Géologie, UMR 5563 - CNRS/IRD/UPS Université de Toulouse, Toulouse, France^b Istituto Nazionale di Geofisica e Vulcanologia - Sezione di Palermo, Italy^c Geological Survey of Japan, AIST - Tsukuba, Japan

ARTICLE INFO

Article history:

Received 23 June 2008

Received in revised form 15 October 2008

Accepted 20 October 2008

Available online xxxx

Editor: R.W. Carlson

Keywords:

Mercury
isotope fractionation
degassing
Vulcano

ABSTRACT

Sampling and analyses methods for determining the stable isotopic compositions of Hg in an active volcanic system were tested and optimized at the volcanic complex of Vulcano (Aeolian Islands, Italy). Condensed gaseous fumarole $\text{Hg}_{(\text{fum})}^{\text{T}}$, plume gaseous elemental $\text{Hg}_{(\text{g})}^{\text{O}}$ and plume particulate $\text{Hg}_{(\text{p})}^{\text{II}}$ were obtained at fumaroles F0, F5, F11, and FA. The average total Hg emissions, based on $\text{Hg}^{\text{T}}/\text{SO}_2$ in condensed fumarolic gases and plumes, range from 2.5 to 10.1 kg yr^{-1} , in agreement with published values [Ferrara, R., Mazzolai, B., Lanzillotta, E., Nucaro, E., Pirrone, N., 2000. Volcanoes as emission sources of atmospheric mercury in the Mediterranean Basin. *Sci. Total Environ.* 259(1–3), 115–121; Aiuppa, A., Bagnato, E., Witt, M.L.L., Mather, T.A., Parello, F., Pyle, D.M., Martin, R.S., 2007. Real-time simultaneous detection of volcanic Hg and SO_2 at La Fossa Crater, Vulcano (Aeolian Islands, Sicily). *Geophys. Res. Lett.* 34(L21307)]. Plume $\text{Hg}_{(\text{p})}^{\text{II}}$ increases with distance from the fumarole vent, at the expense of $\text{Hg}_{(\text{g})}^{\text{O}}$ and indicates significant in-plume oxidation and condensation of fumarole $\text{Hg}_{(\text{fum})}^{\text{T}}$.

Relative to the NIST SRM 3133 Hg standard, the stable isotopic compositions of Hg are $\delta^{202}\text{Hg}_{(\text{fum})}^{\text{T}} = -0.74\% \pm 0.18$ (2SD, $n=4$) for condensed gaseous fumarole $\text{Hg}_{(\text{fum})}^{\text{T}}$, $\delta^{202}\text{Hg}_{(\text{g})}^{\text{O}} = -1.74\% \pm 0.36$ (2SD, $n=1$) for plume gaseous elemental $\text{Hg}_{(\text{g})}^{\text{O}}$ at the F0 fumarole, and $\delta^{202}\text{Hg}_{(\text{p})}^{\text{II}} = -0.11\% \pm 0.18$ (2SD, $n=4$) for plume particulate $\text{Hg}_{(\text{p})}^{\text{II}}$. The enrichment of $\text{Hg}_{(\text{p})}^{\text{II}}$ in the heavy isotopes and $\text{Hg}_{(\text{g})}^{\text{O}}$ in the light isotopes relative to the total condensed fumarolic $\text{Hg}_{(\text{fum})}^{\text{T}}$ gas complements the speciation data and demonstrates a gas-particle fractionation occurring after the gas expulsion in ambient T° atmosphere. A first order Rayleigh equilibrium condensation isotope fractionation model yields a fractionation factor $\alpha_{\text{cond-gas}}$ of 1.00135 ± 0.00058 .

© 2008 Elsevier B.V. All rights reserved.

1. Introduction

Mercury (Hg) is a heavy metal of great concern due to both its extreme mobility and biotoxicity (Lamborg et al., 2003). At present total anthropogenic emissions are estimated to be 2200 Mg yr^{-1} (Pacyna et al., 2006; Wilson et al., 2006), while primary land and ocean emissions are estimated at 500 and 400 Mg yr^{-1} respectively (Selin et al., 2008). Two recent reviews narrow down previous estimates of volcanic Hg emissions of 0.6–830 Mg yr^{-1} (Varekamp and Buseck, 1986; Nriagu and Pacyna, 1988; Ferrara et al., 2000) to 112 Mg yr^{-1} and 700 Mg yr^{-1} (Nriagu and Becker, 2003; Pyle and Mather, 2003). Volcanic Hg emissions may thus represent 12–78% of natural emissions and approximately 4–23% of total global emissions. Even on regional scales, such as the contribution of Mediterranean volcanic emissions to the global atmospheric Hg budget, controversy exists with the impact being estimated as negligible (Ferrara et al., 2000) to important (Pyle and Mather, 2003; Bagnato et al., 2007). A recent global 3D model of atmospheric mercury (GEOS-Chem), including a coupled ocean model, neglects volcanic emissions due to the above

cited uncertainties (Strode et al., 2007; Selin et al., 2008). There is therefore a continuing need for precise estimates of the volcanic Hg budget both at regional and global scales. Equally important is the speciation of volcanic Hg in the fumarolic gases and during the evolution of volcanic plumes. Few volcanic studies simultaneously document gaseous elemental mercury ($\text{Hg}_{(\text{g})}^{\text{O}}$), reactive gaseous mercury ($\text{Hg}_{(\text{g})}^{\text{II}}$), and particulate mercury emission ($\text{Hg}_{(\text{p})}$) (Pyle and Mather, 2003; Bagnato et al., 2007). Volatile Hg species transformation during plume evolution, such as oxidation, reduction and condensation, as a function of temperature and physicochemical gradients remains largely undocumented. In this study we explore the variations in Hg stable isotopic composition of volcanic emissions at Vulcano (Italy), in order to assess species transformations.

Experimental fractionation of Hg isotopes trails their discovery by Aston (1920) by only 1 year and relied on precise density measurements (Brønsted and Hevesy, 1920). Eighty years later, the search for natural terrestrial variations in Hg isotope abundances has become possible with the development of cold vapor – multiple collection ICPMS (CV-MC-ICP-MS, (Klaue et al., 2000)). CV-MC-ICPMS has propelled recent studies on natural Hg stable isotope variations (or the absence thereof) in meteorites (Lauretta et al., 2007), cinnabars (Hintelmann and Lu, 2003), hydrothermal fluids and deposits (Smith

* Corresponding author.

E-mail address: zambardi@lmtg.obs-mip.fr (T. Zambardi).

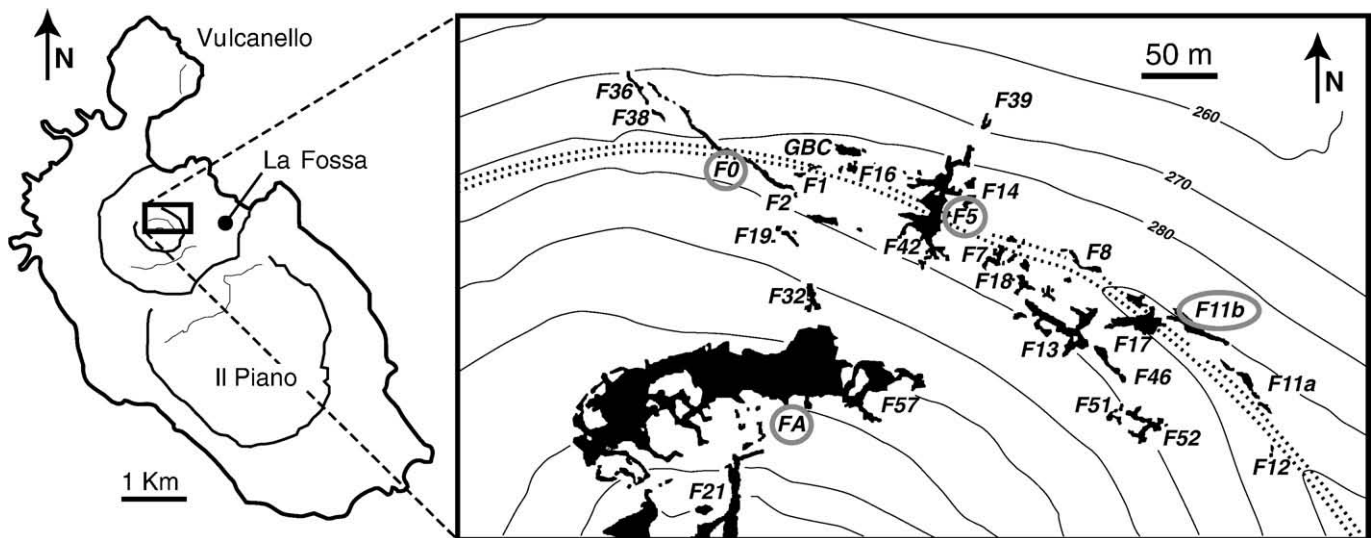


Fig. 1. Map of the La Fossa crater fumarolic field, adapted from Toutain et al. (2003). The dark area means the fumarolic field. The sampled fumaroles F0, F5, F11 and FA are circled.

et al., 2005, 2008), biological samples (Xie et al., 2005), sediments (Foucher and Hintelmann, 2004), and during processes such as microbial reduction (Kritee et al., 2007), volatilization (Zheng et al., 2007) and photoreduction (Bergquist and Blum, 2007). The natural variation in Hg isotopic compositions ranges from $\delta^{202}\text{Hg}$ of -4.5% to $+2.5\%$, relative to the standard NIST SRM 3133, which is defined as $\delta^{202}\text{Hg}=0$. Such a large range of isotopic compositions for a heavy element is not easily explained by mass-dependent equilibrium fractionation, and has in addition to open system Rayleigh-type fractionation recently invoked alternative mechanisms such as non-mass dependent nuclear volume fractionation (Schauble, 2007).

Mass-dependent fractionation of heavy metal isotopes has been observed at the volcano-atmosphere interface for moderately volatile elements such as Zn (Toutain et al., 2008) and Tl (Rehkämper et al., 2007). Toutain et al. (2008) found that Zn in condensed solids is enriched by up to $+1.63\%$ in the heavy Zn isotopes during gas condensation at $590\text{--}293\text{ }^\circ\text{C}$ fumaroles at Merapi Volcano (Indonesia). The Zn observations were explained by a Rayleigh fractionation model with a temperature dependent equilibrium fractionation factor. Physical kinetic isotope fractionation during laboratory evaporation/condensation experiments at low to high temperatures ($5\text{--}1900\text{ }^\circ\text{C}$) has been demonstrated for the elements Hg (Brønsted and Hevesy, 1920; Mulliken and Harkins, 1922; Estrade et al., 2007) and Cd (Wombacher, 2004). The same mechanism has also been invoked to explain high temperature industrial isotope fractionation of Cd and Zn in incinerators and refineries (Cloquet et al., 2006; Sonke et al., 2008). Therefore, both equilibrium and kinetic isotope fractionation mechanisms can be expected to accompany high temperature phase and redox changes under volcanic conditions.

Vulcano (Aeolian Islands, Italy) is a passively degassing volcano which is often used as a natural laboratory for methodological developments (Toutain et al., 2003; Aiuppa et al., 2005, 2007). Permanent fumarolic activity allows easy access to volcanic gases within a range of temperature conditions ($272\text{--}460\text{ }^\circ\text{C}$ for this study). Compared to the other Mediterranean active volcanoes, Vulcano is a low volatile generator with a SO_2 flux (ΦSO_2) estimated at 15 Mg d^{-1} , (Aiuppa et al., 2007), versus $170\text{ to }820\text{ Mg d}^{-1}$ (Allard et al., 2000), and $1000\text{ to }25,000\text{ Mg d}^{-1}$ (Bruno et al., 2001), for Stromboli and Mt Etna respectively. The aim of this work is 1) to validate sampling and analytical methods for Hg stable isotope determinations, 2) determine the Hg emission flux (ΦHg) at Vulcano and compare it with previous estimates, and 3) characterize the Hg stable isotopic composition of fumarole and plume emissions and discuss the potential fractionation processes at the fumarole-atmosphere interface.

2. Sampling methods

Samples were collected in January 2007, under constant dry meteorological conditions. We sampled gas condensates, bulk gases and a gas-aerosol mixture in plumes issuing from the main fumaroles (F0, F5, F11 and FA) with temperatures of $272\text{ }^\circ\text{C}$, $330\text{ }^\circ\text{C}$, $460\text{ }^\circ\text{C}$ and $327\text{ }^\circ\text{C}$ respectively. The fumarolic field is located on the north side of La Fossa crater. F0, F5 and F11 are linked to preexisting faults along the northern rim whereas FA is located on the internal flank of the crater

Table 1

Summary of physico-chemical parameters at Vulcano fumaroles F0, F5, F11 and FA for this study

Site	F0	F5	F11	FA	Average
Fumarole $T\text{ }^\circ\text{C}$	272	330	460	327	347
$\text{SO}_2/\text{H}_2\text{S}$	1.27	1.69	3.43	2.54	2.23
<i>Fumarolic gas</i>					
Total condensate sampled (g)	116	143	76	98	–
Total Hg sampled (ng)	784	1385	756	556	–
[Hg] in condensate (ppb)	6,8	9,7	9,9	5,7	–
Non condensable Hg (ng)	–	76	–	–	–
[Cl] in condensate (wt.%)	1.22	1.99	1.74	1.26	–
Hg/Cl (molar)	9.8×10^{-8}	8.6×10^{-8}	1.0×10^{-7}	8.0×10^{-8}	–
[HCl] (mol%)	0.41	0.34	0.62	0.66	–
$\text{S}^{\text{T}}/\text{Cl}$ (molar)	1.19	0.91	0.69	0.59	–
[Hg] gas $\mu\text{g m}^{-3}$	2.4	3.3	2.6	1.8	2.5
$\text{Hg}_{(\text{fum})}^{\text{T}}/\text{SO}_2$ (mass)	4.6×10^{-7}	4.7×10^{-7}	5.9×10^{-7}	5.9×10^{-7}	5.3×10^{-7}
$\text{Hg}_{(\text{fum})}^{\text{T}}/\text{S}^{\text{T}}$ (mass)	5.1×10^{-7}	5.9×10^{-7}	9.1×10^{-7}	8.5×10^{-7}	7.2×10^{-7}
$\text{Hg}_{(\text{fum})}^{\text{T}}/\text{SO}_2$ (molar)	1.5×10^{-7}	1.5×10^{-7}	1.9×10^{-7}	1.9×10^{-7}	1.7×10^{-7}
$\text{Hg}_{(\text{fum})}^{\text{T}}/\text{S}^{\text{T}}$ (molar)	8.2×10^{-8}	9.4×10^{-8}	1.5×10^{-7}	1.4×10^{-7}	1.1×10^{-7}
Hg flux (kg y^{-1})	2.5	2.6	3.2	3.3	3
<i>Plume</i>					
[GEM] (ng m^{-3})	107	<1	4	4	–
$\text{Hg}_{(\text{p})}^{\text{II}}$ (ng m^{-3})	65	125	69	84	–
$\text{Hg}_{(\text{plume})}^{\text{I}}$ (ng m^{-3})	172	125	73	88	–
$\text{S}^{\text{T}}/\text{Cl}$ (molar)	0.96	0.83	0.6	0.97	–
Hg/Cl (molar)	3.2×10^{-7}	1.1×10^{-7}	8.6×10^{-8}	1.4×10^{-7}	–
$\text{Hg}_{(\text{plume})}^{\text{T}}/\text{SO}_2$ (mass)	1.8×10^{-6}	6.4×10^{-7}	5.8×10^{-7}	6.4×10^{-7}	9.3×10^{-7}
$\text{Hg}_{(\text{plume})}^{\text{T}}/\text{S}^{\text{T}}$ (mass)	2.1×10^{-6}	8.0×10^{-7}	8.9×10^{-7}	9.2×10^{-7}	1.2×10^{-6}
$\text{Hg}_{(\text{plume})}^{\text{T}}/\text{SO}_2$ (molar)	5.9×10^{-7}	2.0×10^{-7}	1.8×10^{-7}	2.0×10^{-7}	3.0×10^{-7}
$\text{Hg}_{(\text{plume})}^{\text{T}}/\text{S}^{\text{T}}$ (molar)	3.3×10^{-7}	1.3×10^{-7}	1.4×10^{-7}	1.5×10^{-7}	1.9×10^{-7}
Hg flux (kg y^{-1})	10.1	3.5	3.1	3.5	5

$\text{SO}_2/\text{H}_2\text{S}$ are calculated for each fumarole from the soda bottles analysis. Fumarole $\text{Hg}^{\text{T}}/\text{S}^{\text{T}}$ are given by combining the $\text{Hg}^{\text{T}}/\text{Cl}$ ratios from the condensates and $\text{S}^{\text{T}}/\text{Cl}$ from the soda bottles. Plume $\text{Hg}^{\text{T}}/\text{Cl}$ is derived from the total Hg (Hg on gold trap+Hg on fiber filters) and chlorine (filter pack) sampled relative to the same measured volume of gas. Plume $\text{S}^{\text{T}}/\text{Cl}$ is given by the Ventury Effect System. Combining both ratios lead to plume $\text{Hg}^{\text{T}}/\text{S}^{\text{T}}$.

(Fig. 1). Gas condensates were sampled at a constant rate (0.8 L min^{-1}) using a quartz tube, quartz connections, an acetone cooled pyrex condenser (Toutain et al., 2008) and acid cleaned 300 mL teflon beaker to collect the condensed liquid phase. Gas condensates typically trap both HCl and the bulk of gaseous trace metals, due to the rapid quenching of hot gas to $\sim 20^\circ\text{C}$. The quenching efficiency was checked for Hg at F5 fumarole by coupling a gold trap at the outlet of the teflon beaker, giving $\text{Hg}_{\text{trap}}/\text{Hg}_{\text{cond}}$.

Bulk fumarole acid gases (HCl , S^{T} ($\text{SO}_2 + \text{H}_2\text{S}$)) were collected by coupling pre-evacuated flasks filled with 4N NaOH to the quartz transfer tube positioned in the fumarole (Sortino et al., 2006). Total $\text{Hg}^{\text{T}}/\text{S}^{\text{T}}$ is derived by combining $\text{Hg}^{\text{T}}/\text{Cl}$ measured in the condensates with $\text{S}^{\text{T}}/\text{Cl}^{\text{T}}$ measured in the soda bottles (Table 1). Volcanic plumes were sampled downwind of the respective vents at ambient air temperatures of ~ 25 to 30°C . Sampling distances were different between F0 fumarole (0.8 to 1 m) and F5, F11 and FA (about 5 to 7 m). Plume $\text{S}^{\text{T}}/\text{Cl}$ ratios were determined using a Venturi Effect Sampler (VES) sampler filled with a 4N NaOH solution and pumping at 9.0 L min^{-1} for 1 h (Toutain et al., 2003). Gaseous Elemental Mercury ($\text{Hg}_{\text{(g)}}^0$ or GEM) in the plume was sampled using gold traps (Brooks Rand Inc., USA) to pre-concentrate $\text{Hg}_{\text{(g)}}^0$ by gold-mercury amalgamation. The gold trap assembly consists of a constricted quartz tube that contains gold coated quartz beads and is preceded by a filter pack composed of in-series particle filter, two alkaline (NaHCO_3) impregnated filters for Cl^{T} trapping, and a soda lime trap to adsorb residual water vapor and $\text{H}_2\text{S}_{\text{(g)}}$. The assembly was operated at a 0.3 L min^{-1} pumping rate for up to 3 h. On one occasion a second gold trap was connected in series in order to monitor potential GEM breakthrough on the first trap, but this proved negligible. Particulate mercury, $\text{Hg}_{\text{(p)}}$ was sampled on pre-combusted 47 mm, $0.2 \mu\text{m}$ glass fiber filters using a parallel pump system running at $6\text{--}7 \text{ L min}^{-1}$ for up to 3 h. The inlets of the parallel GEM and $\text{Hg}_{\text{(p)}}$ filter assemblies were not more than 10 cm apart and operated over the same period of time to avoid bias due to short-term temporal emission and spatial concentration variations (Aiuppa et al., 2007).

3. Analytical methods

3.1. Elemental analyses

The 4N NaOH soda bottles were analysed by HPLC following Sortino et al. (2006). S and Cl contents of condensates, alkaline filters and VES samples were analysed by liquid chromatography (Dionex ICS 2000 HPLC). Selected gold traps were analysed by Atomic Fluorescence Spectrophotometry (Brook Rand Model III, USA) with procedural blanks $<30 \text{ pg}$.

3.2. Hg stable isotope analyses

The acid condensates were first slowly evaporated at 50°C and then digested in concentrated aqua regia (2:3 $\text{HNO}_3:\text{HCl}$) in the same teflon beaker used for collection. This allows full dissolution of metal-bearing sulphur phases which commonly precipitate upon cooling during the sampling procedure (Fischer et al., 1998). A control sample with similar SO_4 and Cl content as the real volcanic condensates was spiked with SRM 3133 Hg standard in order to monitor potential Hg loss and associated isotopic fractionation during evaporation. Quartz fiber filters for $\text{Hg}_{\text{(p)}}$ analyses were leached in concentrated aqua regia.

3.2.1. CV-MC-ICP-MS

Hg concentrations and isotopic compositions of gas condensate and particulate filters digests were analyzed by CV-MC-ICP-MS using a Perkin Elmer (FIAS-400) cold vapor generator coupled to a Thermo Finnigan Neptune at the Laboratoire des Mécanismes et Transferts en Géologie (LMTG, Toulouse, France). Operating conditions are given in Sonke et al. (2008). Concentrated aqua regia digests containing inorganic Hg^{2+} were diluted and on-line reduced with 3% w/v SnCl_2

(Alfa Aesar NormaPur) in 1 N double-distilled HCl. Mass bias drift was monitored using NIST SRM 997 Thallium as internal standard. Thallium was continuously introduced by a desolvation system (CETAC Aridus II) for on-line mass bias correction using the Russel's exponential law (Eq. (1)):

$$r_i = R_i \left(\frac{M_i}{M_k} \right)^\beta$$

where r_i is the corrected isotope ratio, R_i is the measured isotope ratio, M_i is the studied isotope mass (^{199}Hg , ^{200}Hg , ^{201}Hg , ^{202}Hg and ^{204}Hg), and M_k is the reference isotope mass (^{198}Hg). International delta-0 standard NIST SRM 3133 was analyzed before and after each sample,

Table 2

Summary of Hg isotopic compositions, in $\delta^{\text{xxx}}\text{Hg}$ (‰ relative to NIST SRM 3133, see Eq. (1))

	$\delta^{199}\text{Hg}$ (‰)	$\delta^{200}\text{Hg}$ (‰)	$\delta^{201}\text{Hg}$ (‰)	$\delta^{202}\text{Hg}$ (‰)	$\Delta^{199}\text{Hg}$ (‰)	$\Delta^{200}\text{Hg}$ (‰)	$\Delta^{201}\text{Hg}$ (‰)
Condensates							
FA	-0.08	-0.28	-0.24	-0.38	0.02	-0.09	0.05
FA	-0.05	-0.08	-0.09	-0.15	-0.01	-0.01	0.02
FA average	-0.06	-0.18	-0.16	-0.27	0.01	-0.05	0.04
FA 2SD	0.03	0.29	0.21	0.32	0.04	0.11	0.04
F0	-0.11	-0.31	-0.5	-0.71	0.07	0.05	0.03
F0	-0.07	-0.4	-0.61	-0.86	0.15	0.03	0.04
F0	-0.17	-0.33	-0.64	-0.8	0.03	0.07	-0.04
F0 average	-0.12	-0.35	-0.58	-0.79	0.08	0.05	0.01
F0 2SD	0.1	0.09	0.14	0.15	0.12	0.04	0.09
F5	-0.32	-0.58	-0.92	-1.09	-0.05	-0.03	-0.1
F5 2SD	0.2	0.54	0.39	0.44	-	-	-
F11	-0.06	-0.26	-0.46	-0.68	0.11	0.08	0.05
F11	-0.12	-0.32	-0.54	-0.67	0.05	0.02	-0.04
F11	-0.04	-0.53	-0.7	-1.03	0.22	-0.02	0.07
F11 average	-0.07	-0.37	-0.57	-0.79	0.13	0.03	0.02
F11 2SD	0.09	0.28	0.25	0.41	0.17	0.10	0.12
Quartz filters ($\text{Hg}_{\text{(p)}}^{\text{II}}$)							
F0	-0.05	-0.07	-0.02	0.1	-0.08	-0.12	-0.1
F0	-0.02	0.03	0.01	-0.12	0.01	0.09	0.1
F0 average	-0.04	-0.02	0	-0.01	-0.04	-0.02	0.01
F0 2SD	0.05	0.14	0.03	0.32	0.13	0.30	0.28
F11	-0.16	-0.14	-0.33	-0.22	-0.11	-0.03	-0.17
F11	-0.04	-0.03	-0.24	-0.3	0.04	0.12	-0.02
F11 average	-0.1	-0.09	-0.29	-0.26	-0.04	0.04	-0.1
F11 2SD	0.16	0.15	0.12	0.1	0.21	0.21	0.21
FA	-0.1	0.03	-0.07	0.02	-0.11	0.02	-0.09
FA	-0.03	-0.01	-0.09	-0.01	-0.03	-0.01	-0.08
FA average	-0.06	0.01	-0.08	0	-0.06	0.01	-0.08
FA 2SD	0.1	0.06	0.03	0.05	0.11	0.04	0.01
F5	0.07	-0.1	-0.02	-0.09	0.09	-0.06	0.05
F5	-0.1	-0.1	-0.07	-0.13	-0.07	-0.04	0.03
F5	0.01	-0.03	-0.03	-0.06	0.03	0	0.02
F5	-0.08	-0.15	-0.22	-0.33	0	0.02	0.03
F5 average	-0.03	-0.1	-0.08	-0.15	0.01	-0.03	0.03
F5 2SD	0.16	0.1	0.18	0.24	0.13	0.07	0.03
Au trap ($\text{Hg}_{\text{(g)}}^0$)							
F0	-0.55	-0.86	-1.52	-1.73	-0.12	0.01	-0.22
2SD (internal precision)	0.32	0.52	0.22	0.36	-	-	-
Standards							
CRPG-F65A	-0.80	-1.75	-2.64	-3.55	0.10	0.04	0.04
2SD	0.10	0.15	0.23	0.28	0.08	0.06	0.07
CRPG-RL24H	0.59	1.29	1.88	2.56	-0.06	0.00	-0.04
2SD	0.06	0.09	0.10	0.12	0.05	0.06	0.06

Individual replicate samples and their means are shown. Only F0 $\text{Hg}_{\text{(g)}}^0$ had sufficient Hg on the gold trap for isotopic analysis. By exception the uncertainty for F5 condensate is estimated as the 2SD internal uncertainty based on 24 cycles of 8 s signal integration ($\sim 5 \text{ ng}$ of Hg), and includes the uncertainty on the NIST bracketing standard. Long term average isotopic composition (‰ relative to NIST SRM 3133) and external reproducibility on two liquid Hg based in-house standards CRPG-F65A and CRPG-RL24H are also mentioned.

and sample-standard concentrations were matched to within 10%. Delta values are expressed according to Blum and Bergquist (2007) (Eq. (2)):

$$\delta^{xxx}\text{Hg} = \left(\frac{\left(\frac{^{xxx}\text{Hg}}{^{198}\text{Hg}} \right)_{\text{sample}}}{\left(\frac{^{xxx}\text{Hg}}{^{198}\text{Hg}} \right)_{\text{SRM3133}}} - 1 \right) \times 1000$$

At the time of analysis, we did not have the secondary reference material UM-Almaden available. We used two liquid Hg based in-house standards CRPG-F65A and CRPG-RL24H to monitor long-term external reproducibility. In the concentration range of the samples (5–20 ng Hg) we measured a $\delta^{202}\text{Hg}$ of $-3.55\% \pm 0.28$ (2SD, $n=30$) for CRPG-F65A and a $\delta^{202}\text{Hg}$ $2.56\% \pm 0.12$ (2SD, $n=10$) for CRPG-RL24H (Table 2). Our more recent long-term (1 year) reproducibility of UM-Almaden on the LMTG Neptune is $-0.51\% \pm 0.17$ (2SD, $n=34$, (Eпов et al., 2008)), in excellent agreement with the published value of -0.54 ± 0.08 (2SD, Blum and Bergquist, 2007). In this study we apply the 0.28‰ 2SD external uncertainty on CRPG-F65A to all samples, unless the sample replication uncertainty was greater than that value.

3.2.2. CVSI-MC-ICP-MS

Gold traps were used to collect and concentrate $\text{Hg}_{(g)}^0$ vapor. The amalgamated $\text{Hg}_{(g)}^0$ is released as a pulse by flash-heating the traps to 500 °C. Direct introduction of the transient $\text{Hg}_{(g)}^0$ pulse into an MC-ICP-

MS however, gives rise to large mass-bias drift on isotope ratios, and degrades internal precision to the per mil level (Evans et al., 2001). In order to avoid this problem we developed an indirect coupling of gold traps to MC-ICP-MS by off-line collecting the $\text{Hg}_{(g)}^0$ vapor from the trap into a large volume syringe, followed by immediate injection of the $\text{Hg}_{(g)}^0$ vapor into the ICP plasma (Sonke et al., 2008). The cold vapor syringe injection (CVSI) method avoids temporal mass bias drift because the $\text{Hg}_{(g)}^0$ is no longer injected as a transient pulse but as a steady-state signal by a programmable syringe pump. CVSI allows sample-standard bracketing by using an in-house $\text{Hg}_{(g)}^0$ vapor standard (calibrated against NIST SRM 3133), and co-introduction of NIST SRM 997 thallium for internal mass bias correction. This results in an external reproducibility of 0.24‰ (2SD) (for details see Sonke et al., 2008). Gaseous $\text{Hg}_{(g)}^0$ collected on gold traps at fumarole plumes F0, F5, F11 and FA were analyzed by CVSI. Because sample $\text{Hg}_{(g)}^0$ contents were unpredictable, only one NIST 3133 standard analysis has been made after the sample, with the standard signal (Volts) matched to the sample signal $\pm 10\%$.

4. Results and discussion

4.1. Hg/S^T , Hg/SO_2 ratios

Analytical results are given in Table 1. Hg concentrations in fumarolic condensates range from 5.7 (FA) to 9.9 (F11) $\mu\text{g Hg/L}$ of condensate, corresponding to 1.8 to 3.3 $\mu\text{g}/\text{m}^3$ of the total fumarolic

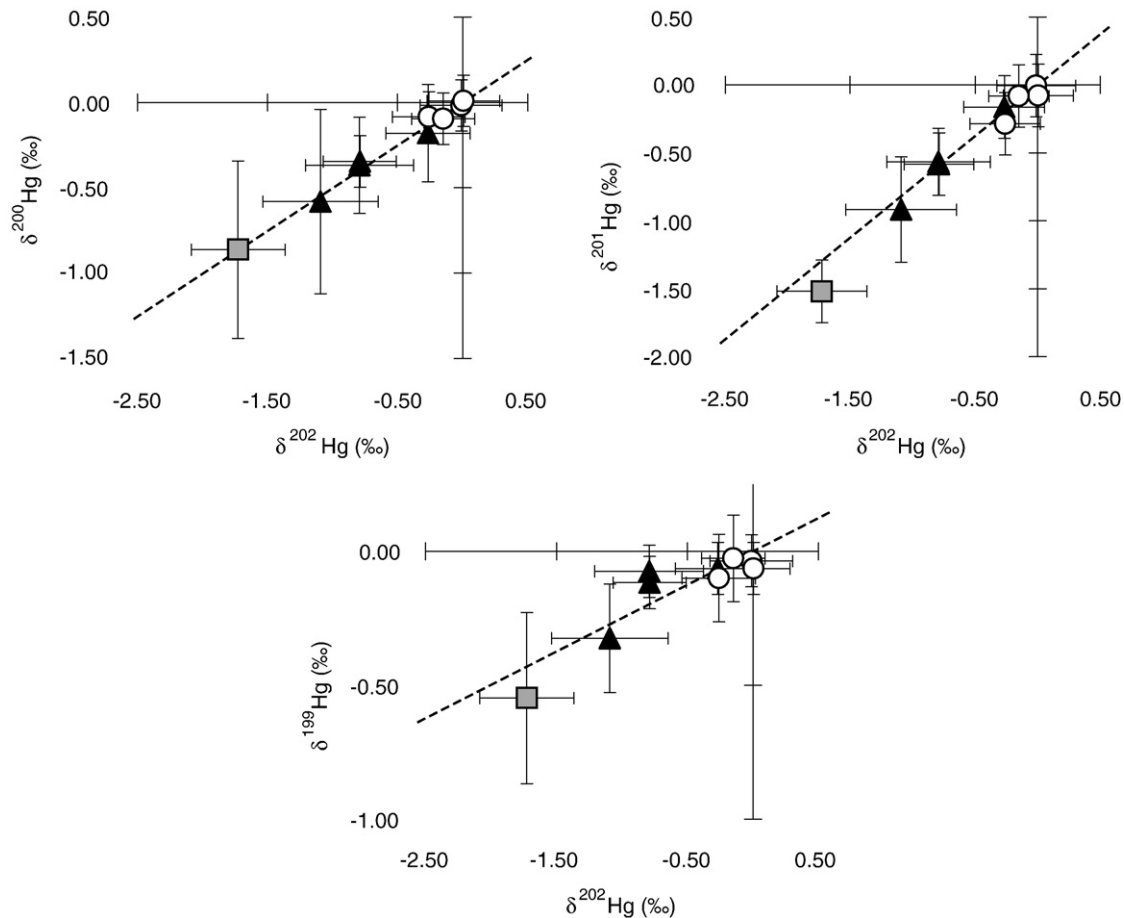


Fig. 2. Three isotope diagrams for all samples analyzed at Vulcano showing residual GEM in F0 plume (gray square), $\text{Hg}_{(p)}^{\text{H}}$ in plumes (white circles), and Hg^{T} in fumaroles (black triangles). The dashed lines mean the predictable mass dependant fractionation (MDF). Within the measurement uncertainties, volcanic Hg emissions and in-plume oxidative condensation do not display evidence of mass independent fractionation (MIF). This potentially renders volcanic Hg emissions discernible from MIF-inducing photochemical processes. (For interpretation of the references to colour in this figure legend, the reader is referred to the web version of this article.)

gas. Non condensable gaseous $\text{Hg}_{(\text{fum})}^{\text{T}}$ was measured at F5 by passing the residual gas at the condenser outlet through a gold trap preceded by a large volume soda lime trap at a constant pumping rate of 0.8 L min^{-1} , and yielded a value of 77 ng Hg trapped on gold, relative to 1385 ng Hg dissolved in the condensate. This suggests an approximate 95% condensation efficiency of total fumarole $\text{Hg}_{(\text{fum})}^{\text{T}}$, similar to published findings by Aiuppa et al. (2007) who achieved 98% condensation at F0 at Vulcano. Total fumarole $\text{Hg}_{(\text{fum})}^{\text{T}}$ can therefore be approximated by $\text{Hg}_{(\text{cond})}^{\text{T}}$, assuming the 5% of non-condensable Hg to be negligible relative to measurement uncertainties. Thermodynamic equilibrium calculations by Aiuppa et al. (2007) suggest that fumarole $\text{Hg}_{(\text{fum})}^{\text{T}}$ at Vulcano is predominantly (99.99%) in the $\text{Hg}_{(\text{g})}^{\text{0}}$ form. Measured $\text{Hg}_{(\text{g})}^{\text{T}}/\text{Cl}$ mass ratios in condensates range from 4.5×10^{-7} to 5.7×10^{-7} , and scaled to the SO_2/Cl ratios of the respective fumaroles lead to $\text{Hg}_{(\text{fum})}^{\text{T}}/\text{SO}_2$ mass ratios of 4.6×10^{-7} to 5.9×10^{-7} (1.5×10^{-7} to 1.9×10^{-7} molar ratios) and to $\text{Hg}_{(\text{fum})}^{\text{T}}/\text{S}^{\text{T}}$ mass ratios of 5.1×10^{-7} to 9.1×10^{-7} (8.2×10^{-8} to 1.5×10^{-7} molar ratios) where S^{T} is $\text{SO}_2 + \text{H}_2\text{S}$ (Table 1). These $\text{Hg}_{(\text{fum})}^{\text{T}}/\text{SO}_2$ are consistent with the observations by Ferrara et al. (2000) and Aiuppa et al. (2007) who found respectively $\text{Hg}_{(\text{g})}^{\text{T}}/\text{S}^{\text{T}}$ mass ratio of 1.16×10^{-7} and $\text{Hg}_{(\text{g})}^{\text{T}}/\text{SO}_2$ mass ratio of 2.9×10^{-6} . Scaling our $\text{Hg}_{(\text{fum})}^{\text{T}}/\text{SO}_2$ ratios in condensates with total SO_2 fluxes measured by spectroscopic methods (15 Mg d^{-1}) during quiescent periods at Vulcano (Aiuppa et al., 2005, 2007), leads to yearly $\text{Hg}_{(\text{fum})}^{\text{T}}$ fluxes of 2.5 to 3.3 kg y^{-1} .

Hg species analyzed in plumes downwind of fumarole vents were gaseous elemental mercury ($\text{Hg}_{(\text{g})}^{\text{0}}$) and particulate mercury ($\text{Hg}_{(\text{p})}^{\text{II}}$). Plume $\text{Hg}_{(\text{p})}^{\text{II}}$ concentrations were at F0: 65 ng m^{-3} , F11: 69 ng m^{-3} , FA: 84 ng m^{-3} , and F5: 125 ng m^{-3} . Plume $\text{Hg}_{(\text{g})}^{\text{0}}$ concentration was significant only for the F0 fumarole (107 ng m^{-3}). At F11, FA and F5, the amount of Hg trapped on gold was lower and close to the detection limit of the CVSI-MC-ICP-MS, and led to concentrations of about 4, 4 and $<1 \text{ ng m}^{-3}$ respectively. Plume

$\text{Hg}_{(\text{plume})}^{\text{T}}/\text{SO}_2$ mass ratios of 5.8×10^{-7} to 1.8×10^{-6} (with $\text{Hg}_{(\text{plume})}^{\text{T}} = \text{Hg}_{(\text{g})}^{\text{0}} + \text{Hg}_{(\text{p})}^{\text{II}}$) are similar to total fumarole $\text{Hg}_{(\text{fum})}^{\text{T}}/\text{SO}_2$ mass ratios of 4.6×10^{-7} to 5.9×10^{-7} and therefore result in comparable yearly Hg fluxes of 3.1 to 10.1 kg y^{-1} . This suggests that at the plume sampling distances ($<10 \text{ m}$) no significant Hg deposition has taken place.

On the contrary, $\text{Hg}_{(\text{p})}^{\text{II}}/\text{Hg}_{(\text{g})}^{\text{0}}$ ratios at the different fumarole plumes are variable and suggest an increase as a function of distance from the vent. The smallest distance (F0, $\sim 1 \text{ m}$) exhibits the lowest $\text{Hg}_{(\text{p})}^{\text{II}}/\text{Hg}_{(\text{g})}^{\text{0}}$ of about 0.6, whereas the largest plume-vent distances (F5, F11 and FA, 5 to 7 m) have the highest $\text{Hg}_{(\text{p})}^{\text{II}}/\text{Hg}_{(\text{g})}^{\text{0}}$. According to the $\text{Hg}_{(\text{g})}^{\text{0}}$ measurement uncertainties, $\text{Hg}_{(\text{p})}^{\text{II}}/\text{Hg}_{(\text{g})}^{\text{0}}$ for F5, F11 and FA cannot be precisely quantified but are expected to be at least 17 times more than the F0 $\text{Hg}_{(\text{p})}^{\text{II}}/\text{Hg}_{(\text{g})}^{\text{0}}$ ratio. This observation suggests that low temperature fumarole $\text{Hg}_{(\text{fum})}^{\text{T}}$ emissions, which are essentially $\text{Hg}_{(\text{g})}^{\text{0}}$ at Vulcano, may be rapidly oxidized within the relatively humid and acidic conditions of the plume environment.

4.2. Hg stable isotopic compositions

The total variation in $\delta^{202}\text{Hg}$ for the Vulcano samples ranges from -1.74% to $+0.01\%$, which is more than six times larger than the external reproducibility on the measurements. Three-isotope diagrams of $\delta^{202}\text{Hg}$ vs. $\delta^{199}\text{Hg}$, $\delta^{200}\text{Hg}$, and $\delta^{201}\text{Hg}$ (Fig. 2) reveal a mass-dependent behavior within the measurement uncertainties for all samples. Total fumarole emissions, $\text{Hg}_{(\text{fum})}^{\text{T}}$ have an average $\delta^{202}\text{Hg}$ of $-0.74\% \pm 0.18$ (2SD, $n=4$). Plume $\text{Hg}_{(\text{p})}^{\text{II}}$ has an average $\delta^{202}\text{Hg}$ of $-0.11\% \pm 0.18$ (2SD, $n=4$) and $\text{Hg}_{(\text{g})}^{\text{0}}$ at F0 has a $\delta^{202}\text{Hg}$ of $-1.74\% \pm 0.36$ (2SD, internal precision, $n=1$) (Fig. 3). The in-plume oxidative condensation of Hg on particulates and acidic aerosols is therefore accompanied by an isotopic fractionation that enriches the oxidized

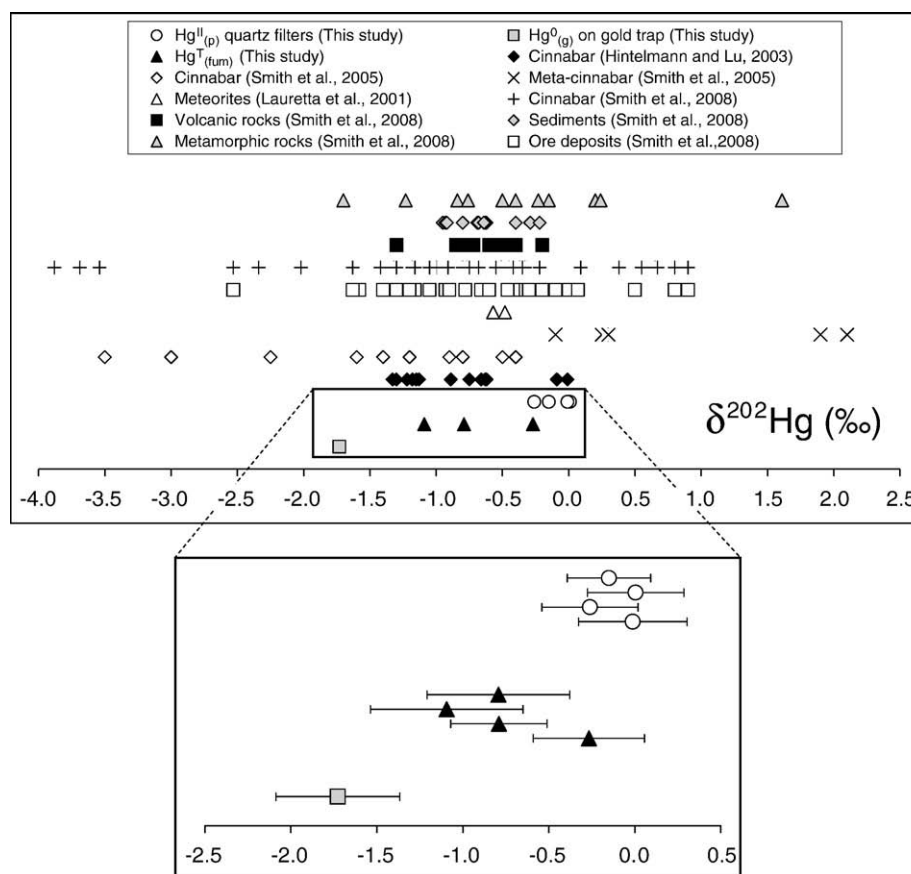


Fig. 3. Comparison of $\delta^{202}\text{Hg}$ (‰) between fumarole $\text{Hg}_{(\text{fum})}^{\text{T}}$, plume $\text{Hg}_{(\text{g})}^{\text{0}}$ and $\text{Hg}_{(\text{p})}^{\text{II}}$ at Vulcano. Selected literature data on Hg isotopic compositions in endogeneous geochemical contexts is also included.

$Hg_{(p)}^{II}$ in the heavy isotopes and the residual $Hg_{(g)}^0$ in the lighter isotopes relative to the $Hg_{(fum)}^T$ emitted at the F0 fumarole. Not enough $Hg_{(g)}^0$ was collected at FA, F5 and F11 to permit isotopic analyses. The sign of fractionation, i.e. heavy isotope enriched condensates, suggests that an equilibrium isotope fractionation mechanisms dominates over potentially present kinetic isotope fractionation. The heavier Hg isotopes become incorporated in a stronger bonding environment, e.g. as $HgCl_{2(aq)}$ in aqueous aerosols, $HgS_{(s)}$ in solids or adsorbed Hg^{II} onto particles. Rapid experimental precipitation of for example Fe from fluids however, has been demonstrated to be mainly governed by kinetic isotope fractionation, opposite from our observations (Beard and Johnson, 2004). Considering the rapidity of the condensation process, it is probable that the fractionation be partially kinetic. Then these results may reflect a composite effect of equilibrium and kinetic fractionation where equilibrium fractionation is dominant. A similar gas-condensate equilibrium isotope fractionation process was recently reported for Zn isotopes in Merapi volcanic gases and condensed solids (Toutain et al., 2008). Using a simple Rayleigh partial condensation model, the evolving isotopic composition of $Hg_{(g)}^0$ and the cumulative oxidized $Hg_{(p)}^{II}$ can be calculated:

$$\delta^{202}Hg_{(g)}^0 = (1000 + \delta^{202}Hg_{(g,initial)}^0) \times f^{(\alpha_{cond-gas}-1)} - 1000 \quad (3)$$

$$\delta^{202}Hg_{(p)}^{II} = (1000 + \delta^{202}Hg_{(g,initial)}^0) \times \frac{(1-f)^{\alpha_{cond-gas}}}{1-f} - 1000 \quad (4)$$

where f is the fraction of residual $Hg_{(g)}^0$, and $\alpha_{cond-gas}$ is the isotope fractionation factor, defined as $(^{202}Hg/^{198}Hg)_{cond}/(^{202}Hg/^{198}Hg)_{gas}$. The 'f' value for the F0 fumarole was calculated following the relation $f = Hg_{(g)}^0 / (Hg_{(p)}^{II} + Hg_{(g)}^0)$. $\alpha_{cond-gas}$ was optimized only for fumarole F0, because all three key parameters, $\delta^{202}Hg_{(g)}^T$, $\delta^{202}Hg_{(g)}^0$, and $\delta^{202}Hg_{(p)}^{II}$ were measured. An optimal fit of the F0 data is obtained for $\alpha_{cond-gas} = 1.00135 \pm 0.00058$ (Fig. 4). Schauble (2007) calculated theoretical, ab initio, mass dependent equilibrium fractionation (MDF) factors between $Hg_{(g)}^0$ vapor and gaseous divalent $Hg_{(g)}^{II}$ species such as $HgCl_{2(g)}$. The theoretically predicted fractionation factor $\alpha_{HgCl_2-Hg^0}^{MDF}$ at 40 °C is ~ 1.001 which is similar to our fitted value. It is of interest to note that Schauble (2007) predicted that an additional mass-independent fractionation (MIF) contribution accompanies the $HgCl_2$ - Hg^0 reaction. The MIF, induced by the nuclear volume effect (nuclear field shift), has a predicted $\alpha_{HgCl_2-Hg^0}^{MIF}$ of 1.00127, such that a total predicted $\alpha_{HgCl_2-Hg^0}^{(MDF+MIF)}$ of 1.00219 ± 0.00030 applies (Schauble, 2007). Nuclear volume fraction-

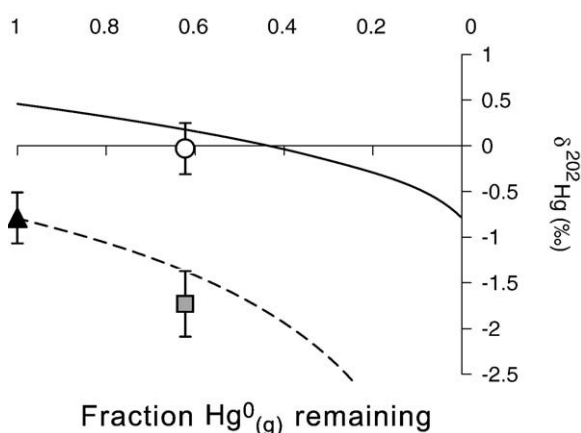


Fig. 4. In-plume Rayleigh condensation model for Hg isotopes at F0 fumarole. The black triangle is the total gas, the white circle is the plume $Hg_{(p)}^{II}$ and the gray square is the plume $Hg_{(g)}^0$. Total Hg isotopic composition is given for $f = 1$ (F0 $\delta^{202}Hg = -0.79\text{‰}$); plume $Hg_{(g)}^0/Hg_{(p)}^{II}$ ratio is 0.62. The effective equilibrium condensation isotope fractionation factor is best constrained with $\alpha_{cond-gas} = 1.00135 \pm 0.00058$. (For interpretation of the references to colour in this figure legend, the reader is referred to the web version of this article.)

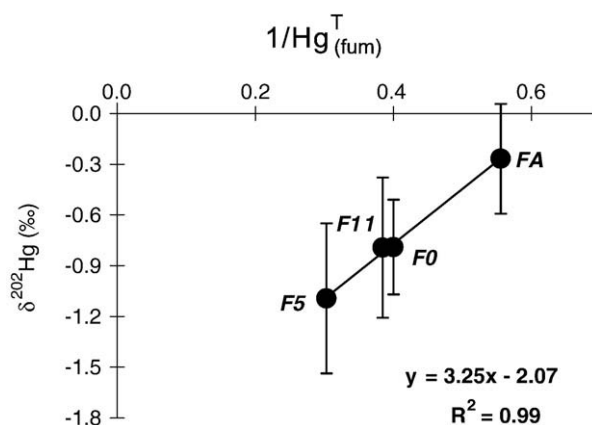


Fig. 5. Inverse $Hg_{(fum)}^T$ concentrations ($L\ ng^{-1}$) correlate linearly with $\delta^{202}Hg$ (‰) ($r^2=0.99$). Following an observation by Nuccio et al. (1999), the correlation likely represents source mixing of a magmatic end member with a hydrothermal end member that enriches the volcanic gases in isotopically light Hg.

ation however, induces deviations from mass dependence for the odd isotopes, notably ^{199}Hg . When our observations at F0 are fitted with the predicted nuclear volume $\alpha_{cond-gas}^{MIF}$ of 1.00127, then the largest MIF $\Delta^{199}Hg$ anomalies (with $\Delta^{199}Hg$ defined as $\delta^{199}Hg - 0.251 \times \delta^{202}Hg$; see (Blum and Bergquist, 2007) that we should have measured are $+0.11\text{‰}$ for $\Delta^{199}Hg_{(g)}^0$ and -0.17‰ for $\Delta^{199}Hg_{(p)}^{II}$. Measured $\Delta^{199}Hg_{(g)}^0$ and $\Delta^{199}Hg_{(p)}^{II}$ are $+0.02\text{‰}$ (no 2SD available), and $-0.04\text{‰} \pm 0.13$ (2SD, Table 2) respectively, suggesting no indication of nuclear volume induced MIF in the F0 samples.

Fumarole $\delta^{202}Hg_{(fum)}^T$ are positively correlated ($r^2=0.99$) with the inverse of $Hg_{(fum)}^T$ concentrations (Fig. 5). This correlation can be the result of reactive processes, such as condensation occurring within the fumarole field or due to mixing of two different gaseous Hg sources. The observations show that lower $Hg_{(fum)}^T$ levels carry higher $\delta^{202}Hg_{(fum)}^T$ signatures (Fig. 5), and suggest a dominant kinetic isotope fractionation mechanism, i.e. a light isotope enriched condensate leaves behind a heavy isotope enriched gas. Such an interpretation is opposite from the predominant equilibrium isotope fractionation occurring in the F0 fumarole plume. Nevertheless, the gradual switch from kinetic isotope fractionation at higher temperatures during gas ascent towards equilibrium isotope fractionation in the fumarole plume was also suggested for Zn isotopes at Merapi Volcano, albeit at higher temperatures (Toutain et al., 2008). Based on carbon dioxide and helium concentrations in the gas phase, Nuccio et al. (1999) demonstrated that two end members (magmatic and hydrothermal) can be deciphered at Vulcano. Their data indicate that FA fumarole gases may be more magmatic in nature, while F0, F5 and F11 gases reflect a more hydrothermal chemical composition. Our data then possibly suggest an enrichment of fumarole gases by hydrothermal Hg. In this case the admixed Hg would either reflect a source that is enriched in the lighter isotopes, and/or the hydrothermal process itself which preferentially mobilizes the lighter isotopes. Hydrothermal mobilization of the lighter Hg isotopes by fluid boiling has been proposed to explain observations of light Hg isotope enriched cinnabar (HgS) in fossil hydrothermal systems (Smith et al., 2005). While this hypothesis suggests a non negligible role of the aquifer on Hg isotopic signatures at Vulcano, it remains inconclusive and more work is needed.

The speciation dynamics of volcanic Hg emissions is an important and generally under-characterized aspect of global Hg emission inventories (Pyle and Mather, 2003). Our observations show that at Vulcano Hg species may undergo modification due to in-plume oxidation of gaseous $Hg_{(g)}^0$. On the global scale, oxidized $Hg_{(g)}^{II}$ and $Hg_{(p)}^{II}$ species have shorter atmospheric residence times (16 and 3 days respectively) than $Hg_{(g)}^0$ (9.5 months) due to efficient wet and dry

scavenging (Selin et al., 2008). The efficient in-plume oxidation of $\text{Hg}_{(g)}^0$ at Vulcano therefore suggests that its Hg emissions are more significant for the regional Hg emission and deposition budget than for the global budget. Aiuppa et al. (2007) have suggested similar oxidative scavenging of $\text{Hg}_{(g)}^0$ at Vulcano's F0 fumarole, sampled at a similar distance of 0.8 m. However, their observations are based on a decrease of the average $\text{Hg}_{(g)}^0/\text{SO}_{2(g)}$ ratio of the plume (mass ratio 1.09×10^{-6}) relative to the fumarole $\text{Hg}_{(fumarole)}^0/\text{SO}_{2(g)}$ mass ratio of 2.9×10^{-6} . Their maximum plume $\text{Hg}_{(g)}^0/\text{SO}_{2(g)}$ ratio observed during a 30 min real-time monitoring of $\text{Hg}_{(g)}^0$ and $\text{SO}_{2(g)}$ fluxes was 2.6×10^{-6} , which is similar to the fumarole emission.

Two Hg speciation measurements in a dilute plume of Etna volcano (Italy) resulted in $\text{Hg}_{(p)}^{\text{II}}/\text{Hg}_{(g)}^0$ mass ratios of 0.4–0.6 (DeDeurwaerder et al., 1982). More recent speciation measurements in near-vent volcanic plumes at Etna indicate much lower $\text{Hg}_{(p)}^{\text{II}}/\text{Hg}_{(g)}^0$ ratios of 0.01 (Bagnato et al., 2007). This incompatibility has been explained to result from higher plume silicate ash content in the early 1980s. Given that Bagnato et al.'s plume ages are on the order of seconds to minutes, and therefore similar to our plume ages at Vulcano (seconds), there appear to be important differences in plume Hg speciation dynamics between Vulcano's fumaroles and Etna's open degassing environment. Ultimately, differences in Hg species evolution during plume aging have to be sought in the physico-chemical properties of plumes. Our study thus reiterates the need for additional field and experimental work on volcanic plumes, and suggests that stable Hg isotopes may provide additional insights.

Within the stated measurement uncertainties, volcanic Hg emissions and in-plume oxidative condensation do not display evidence of mass independent fractionation (Fig. 2). In the context of global and regional Hg cycling and emissions inventories, this suggests that natural volcanic emissions may potentially be discerned from aquatic photochemical Hg evasion (Bergquist and Blum, 2007) by their respective absence and presence of MIF anomalies. It also appears that endogenous geochemical processes in general, i.e. hydrothermalism, volcanism, crust formation, ore formation etc. (Hintelmann and Lu, 2003; Smith et al., 2005, 2008), are characterized by mass dependent fractionation processes only.

5. Conclusions

In this study and a related publication (Sonke et al., 2008) we showed that it is now feasible to measure the isotopic composition of atmospheric Hg, based on the use of standard analytical equipment (gold traps). At Vulcano Island we measured Hg emissions and isotopic signatures, with the following results:

1. Average fumarole total $\text{Hg}_{(g)}^{\text{T}}/\text{SO}_{2(g)}$ mass ratios of 5.3×10^{-7} that are similar to plume $\text{Hg}_{(g)}^{\text{T}}/\text{SO}_{2(g)}$ mass ratios of 9.3×10^{-7} , and translate into an averaged Hg emission budget of 4.0 kg yr^{-1} , in agreement with published emissions (Ferrara et al., 2000; Aiuppa et al., 2007).
2. Significant in-plume oxidative condensation of gaseous $\text{Hg}_{(g)}^0$ into particulate $\text{Hg}_{(p)}^{\text{II}}$. Across four different fumaroles, more than 90% of Hg appears to be oxidized over a short distance (<10 m).
3. The oxidative condensation of gaseous $\text{Hg}_{(g)}^0$ is accompanied by equilibrium Hg isotope fractionation with $\alpha_{\text{cond-gas}}$ of 1.00135 ± 0.00058 (optimized for F0). Relative to fumarole $\text{Hg}_{(g)}^{\text{T}}$ with $\delta^{202}\text{Hg}$ of -0.79% , $\text{Hg}_{(p)}^{\text{II}}$ becomes enriched in the heavier isotopes, leaving residual $\text{Hg}_{(g)}^0$ enriched in the lighter isotopes.
4. Within the stated measurement uncertainties, volcanic Hg emissions and in-plume oxidative condensation do not display evidence of mass independent fractionation (MIF).

Acknowledgements

The following people are warmly acknowledged: Bernard Reynier for field assistance, Remy Freydier for analytical assistance on the

LMTG Neptune, Maïte Carayon for HPLC analyses and Christiane Cavare-Hester for drawings. This work has been funded by Marie Curie grant MEIF-CT-2004-011207 to JES and the French CNRS. Joel Blum and Alessandro Aiuppa are thanked for their constructive reviews.

References

- Aiuppa, A., Inguaggiato, S., McGonigle, A.J.S., O'Dwyer, M., Oppenheimer, C., Padgett, M.J., Rouwet, D., Valenza, M., 2005. H₂S fluxes from Mt. Etna, Stromboli, and Vulcano (Italy) and implications for the sulfur budget at volcanoes. *Geochim. Cosmochim. Acta* 64, 1861–1871.
- Aiuppa, A., Bagnato, E., Witt, M.L.I., Mather, T.A., Parello, F., Pyle, D.M., Martin, R.S., 2007. Real-time simultaneous detection of volcanic Hg and SO₂ at La Fossa Crater, Vulcano (Aeolian Islands, Sicily). *Geophys. Res. Lett.* 34 (L21307).
- Allard, P., Aiuppa, A., Loyer, H., Carrot, F., Gaudry, A., Pinte, G., Michel, A., Dongarra, G., 2000. Acid gas and metal emission rates during long lived basalt degassing at Stromboli. *Geophys. Res. Lett.* 27 (8), 1207–1210.
- Aston, F.W., 1920. Isotopes and atomic weights. *Nature* 105, 617.
- Bagnato, E., Aiuppa, A., Parello, F., Calabrese, S., D'Alessandro, W., Mather, T.A., McGonigle, A.J.S., Pyle, D.M., Wängberg, I., 2007. Degassing of gaseous (elemental and reactive) and particulate mercury from Mount Etna Volcano (Southern Italy). *Atmos. Environ.* 41, 7377–7388.
- Beard, B.L., Johnson, C.M., 2004. Fe isotope variation in the modern and ancient earth and other planetary bodies. In: Johnson, C.M., Beard, B.L., Albarède, F. (Eds.), *Geochemistry of Non Traditional Stable Isotopes*, pp. 319–357.
- Bergquist, B.A., Blum, J.D., 2007. Mass-dependant and independent fractionation of Hg isotopes by photoreduction in aquatic systems. *Science* 318, 417–420.
- Blum, J.D., Bergquist, B.A., 2007. Reporting of variations in the natural isotopic composition of mercury. *Anal. Bioanal. Chem.* 388, 353–359.
- Brønsted, J.N., Hevesy, G.V., 1920. The separation of the isotopes of the mercury. *Nature* 106, 144.
- Bruno, N., Caltabiano, T., Giammanco, S., Romano, R., 2001. Degassing of SO₂ and CO₂ at Mt Etna (Sicily) as an indicator of pre-eruptive ascent and shallow emplacement of magma. *J. Volcanol. Geotherm. Res.* 143, 110–137.
- Cloquet, C., Carignan, J., Libourel, G., 2006. Isotopic composition of Zn and Pb atmospheric depositions in an urban/periurban area of northeastern France. *Environ. Sci. Technol.* 40, 6594–6600.
- DeDeurwaerder, H., Decadt, G., Baeyens, W., 1982. Estimation of mercury fluxes by Mount Etna Volcano. *Bull. Volcanol.* 45 (3), 191–196.
- Epov, V.N., Rodriguez-Gonzalez, P., Sonke, J.E., Tessier, E., Amouroux, D., Maurice Bourgoïn, L., Estrade, N., Carignan, J., Donard, O.F.X., 2008. Measurement of Hg isotopic ratios on molecular level using GC-MC-ICPMS hyphenation. *Geophys. Res. Abstr.* 10, EGU 2008-A-025.
- Estrade, N., Carignan, J., Sonke, J.E., Donard, O.F.X., 2007. Donard, mass independent fractionation of Hg isotopes during evaporation and condensation processes. *Geochim. Cosmochim. Acta* 71, A262–A262.
- Evans, R.D., Hintelmann, H., Dillon, P.J., 2001. Measurement of high precision isotope ratios for mercury from coals using transient signals. *J. Anal. At. Spectrom.* 16, 1064–1069.
- Ferrara, R., Mazzolai, B., Lanzillotta, E., Nucaro, E., Pirrone, N., 2000. Volcanoes as emission sources of atmospheric mercury in the Mediterranean Basin. *Sci. Total Environ.* 259 (1–3), 115–121.
- Fischer, T.P., Shuttleworth, S., O'Day, P.A., 1998. Determination of trace and platinum-group elements in high ionic strength volcanic fluids by sector field inductively coupled plasma mass spectrometry (ICP-MS). *J. Anal. Chem.* 362, 457–464.
- Foucher, D., Hintelmann, H., 2004. High precision measurement of mercury isotope ratios in sediments using cold vapor generation MC-ICP-MS. *Anal. Bioanal. Chem.* 384, 1470–1478.
- Hintelmann, H., Lu, S.Y., 2003. High precision isotope ratio measurements of mercury isotopes in cinnabar ores using multi-collector inductively coupled plasma mass spectrometry. *Analyst* 128, 635–639.
- Klaue, S.E., Kesler, E., Blum, J.D., 2000. International Conference on Heavy Metals in the Environment, Ann Arbor, MI, USA.
- Kritee, K., Blum, J.D., Johnson, M.W., Bergquist, B.A., Barkay, T., 2007. Mercury stable isotope fractionation during reduction of Hg(II) to Hg(0) by mercury resistant microorganisms. *Environ. Sci. Technol.* 41, 1889–1895.
- Lamborg, C.H., Tseng, C.M., Fitzgerald, W.F., Balcom, P.H., Hammerschmidt, C.R., 2003. Determination of the mercury complexation characteristics of dissolved organic matter in natural waters with “reducible Hg” titrations. *Environ. Sci. Technol.* 37, 3316–3322.
- Lauretta, D.S., Klaue, B., Blum, J.D., Buseck, P.R., 2007. Mercury abundances and isotopic compositions in the Murchison (CM) and Allende (CV) carbonaceous chondrites. *Geochim. Cosmochim. Acta* 65, 2807–2818.
- Mulliken, Harkins, 1922. The separation of isotopes. Theory of resolution of isotopic mixtures by diffusion and similar processes. Experimental separation of mercury by evaporation in a vacuum. *J. Am. Chem. Soc.* 44, 37–65.
- Nriagu, J., Becker, C., 2003. Volcanic emissions of mercury to the atmosphere: global and regional inventories. *Sci. Total Environ.* 304, 3–12.
- Nriagu, J.O., Pacyna, J.M., 1988. Quantitative assessment of worldwide contamination of air water and soils by trace-metals. *Nature* 333, 134–139.
- Nuccio, P.M., Paonita, A., Sortino, F., 1999. Geochemical modeling of mixing between magmatic and hydrothermal gases: the case of Vulcano Island. *Earth Planet. Sci. Lett.* 167, 321–333.

- Pacyna, E.G., Pacyna, J.M., Steenhuisen, F., Wilson, S., 2006. Global anthropogenic mercury emission inventory for 2000. *Atmos. Environ.* 40, 4048–4063.
- Pyle, D.M., Mather, T.A., 2003. The importance of volcanic emissions for the global atmospheric mercury cycle. *Atmos. Environ.* 37, 5115–5124.
- Rehkämper, M., Baker, R.G.A., Nielsen, S.G., Hinkley, T.K., Toutain, J.P., 2007. Volcanic outgassing and the Tl isotope composition of the oceans. *Geochim. Cosmochim. Acta* 71, A827.
- Schauble, E.A., 2007. Role of nuclear volume in driving equilibrium stable isotope fractionation of mercury, thallium, and other very heavy elements. *Geochim. Cosmochim. Acta* 71, 2170–2189.
- Selin, N.E., Jacob, D.J., Park, R.J., Yantosca, R.M., Strode, S.A., Jaeglé, L., Jaffé, D., 2008. Chemical cycling and deposition of atmospheric mercury: global constraints from observations. *J. Geophys. Res.* 112.
- Smith, C.N., Kesler, E., Klaue, B., Blum, J.D., 2005. Mercury isotope fractionation in fossil hydrothermal systems. *Geology* 33, 825–828.
- Smith, C.N., Kesler, S.E., Blum, J.D., Rytuba, J.J., 2008. Isotope geochemistry of mercury in source rocks, mineral deposits and spring deposits of the California Coast Ranges, USA. *Earth Planet. Sci. Lett.* 269, 399–407.
- Sonke, J.E., Zambardi, T., Toutain, J.P., 2008. Indirect gold trap MC-ICP-MS coupling for Hg stable isotope analysis using a syringe injection interface. *J. Anal. At. Spectrom.* 23, 569–573.
- Sortino, F., Nonell, A., Toutain, J.P., Munoz, M., Valladon, M., Volpicelli, G., 2006. A new method for sampling fumarolic gases: analysis of major, minor and metallic trace elements with ammonia solutions. *J. Volcanol. Geotherm. Res.* 158, 244–256.
- Strode, S.A., Jaeglé, L., Selin, N.E., Jacob, D.J., Park, R.J., Yantosca, R.M., Mason, R.P., Slemr, F., 2007. Air-sea exchange in the global mercury cycle. *Glob. Biogeochem. Cycles* 21.
- Toutain, J.P., Sortino, F., Reynier, B., Dupre, B., Munoz, M., Nonell, A., Polve, M., Vale, S.C.d., 2003. A new collector for sampling volcanic aerosols. *J. Volcanol. Geotherm. Res.* 123, 95–103.
- Toutain, J.P., Sonke, J., Munoz, M., Nonell, A., Polvé, M., Viers, J., Freydier, R., Sortino, F., Joron, J.L., Sumarti, S., 2008. Evidence for Zn isotopic fractionation at Merapi Volcano. *Chem. Geol.* 253, 74–82.
- Varekamp, C.V., Buseck, P.R., 1986. Global mercury flux from volcanic and geothermal sources. *Appl. geochem.* 1, 65–73.
- Wilson, S.J., Steenhuisen, F., Pacyna, J.M., Pacyna, E.G., 2006. Mapping the spatial distribution of global anthropogenic mercury atmospheric emission inventories. *Atmos. Environ.* 40, 4621–4632.
- Wombacher, F., 2004. Determination of the mass-dependence of cadmium isotope fractionation during evaporation. *Geochim. Cosmochim. Acta* 68, 2349–2357.
- Xie, Q.L., Lu, S.Y., Evans, D., Dillon, P., Hintelmann, H., 2005. High precision Hg isotope analysis of environmental samples using gold trap-MC-ICP-MS. *J. Anal. At. Spectrom.* 20, 515–522.
- Zheng, W., Foucher, D., Hintelmann, H., 2007. Mercury isotope fractionation during volatilization of Hg(0) from solution into the gas phase. *J. Anal. At. Spectrom.* 22, 1097–1104.